Pulse shaping via Backward Second Harmonic Generation

Matteo Conforti, Costantino de Angelis, Usman K Sapaev, Gaetano Assanto

Pulse shaping via Backward Second Harmonic Generation

Matteo Conforti and Costantino De Angelis

Dept. of Electronics for Automation, University of Brescia, via Branze 38, 25123 Brescia, Italy

deangeli@ing.unibs.it - http://nora.ing.unibs.it

Usman K. Sapaev and Gaetano Assanto

NooEL- University "Roma Tre", Via della Vasca Navale 84, 00146 Rome, Italy

assanto@uniroma3.it - http://optow.ele.uniroma3.it/

Abstract: We numerically demonstrate pulse shaping by backward frequency doubling of femtosecond laser pulses in engineered quasi-phase-matched waveguides. We employ optimal control theory to access the regime of pump depletion.

OCIS codes: (190.2620) Harmonic generation and mixing; (190.4410) Nonlinear optics, parametric processes, (320.5540) Pulse shaping.

References and links

1. D. W. McCamant, P. Kukura, S. Yoon, and R. A. Mathies, "Theory of femtosecond stimulated Raman spectroscopy," Rev. Sci. Instrum. **71**, 4971-4976 (2004).
2. P. Kukura, D. W. McCamant, S. Yoon, D. B. Wandschneider, and R. A. Mathies, "Structural observation of the primary isomerization in vision with femtosecond-stimulated Raman," Science **310**, 1006-1011 (2005).
3. A. M. Weiner, "Femtosecond optical pulse shaping and processing," Prog. Quant. Electron. **19**, 161-237 (1995).
4. M. Lauritano, A. Parini, G. Bellanca, S. Trillo, M. Conforti, A. Locatelli, and C. De Angelis, "Bistability, limiting, and self-pulsing in backward SHG: a time-domain approach," J. Opt. A: Pure Appl. Opt. **8**, S494-S501 (2006).
5. C. Conti, S. Trillo, and G. Assanto, "Energy localization in photonic crystals of a purely nonlinear origin," Phys. Rev. Lett. **85**, 2502-2505 (2000).
6. K. Gallo, P. Baldi, M. De Micheli, D. B. Ostrowsky, and G. Assanto, "Cascading phase-shift and multivalued response in counterpropagating frequency nondegenerate parametric amplifiers," Opt. Lett. **25**, 966-968 (2000).
7. F. Laurell, C. Canalias, and V. Pasiskevicius, "Periodically poled crystals with submicrometer grating- fabrication, evolution and application," EOS Top. Meet. on Optical Microsystems (Capri, Sept. 2005)
8. A. C. Busacca, A. C. Cino, S. Riva Sanseverino, M. Ravaro, and G. Assanto, "Silica masks for improved surface poling of lithium niobate," Electron. Lett. **41**, 92-94 (2005).
9. A. C. Busacca, R. L. Oliveri, A. C. Cino, S. Riva-Sanseverino, A. Parisi, and G. Assanto, "Ultraviolet Quasi-Phase-Matched Second Harmonic Generation in Surface Periodically Poled Lithium Niobate Optical Waveguides," Laser Phys. **17**, 884-888 (2007).
10. C. Canalias and V. Pasiskevicius, "Mirrorless optical parametric oscillator", Nat. Photon. **1**, 459-462 (2007).
11. S. E. Harris, "Proposed Backward Wave Oscillation in the Infrared," Appl. Phys. Lett. **9**, 114-116 (1966).
12. P. St. J. Russell, "Theoretical study of parametric frequency and wavefront conversion in nonlinear holograms," IEEE J. Quantum Electron. **27**, 830-835 (1991).
13. M. Conforti, A. Locatelli, C. De Angelis, A. Parini, G. Bellanca, and S. Trillo, "Self-pulsing instabilities in backward parameric wave mixing," J. Opt. Soc. Am. B **22**, 2178-2184 (2005).
14. G. D'Alessandro, P. St. J. Russell, and A. A. Wheeler, "Nonlinear dynamics of a backward quasi-phase-matched second-harmonic generator," Phys. Rev. A **55**, 3211-3218 (1997).
15. C. Conti, G. Assanto, and S. Trillo, "Cavityless oscillations through backward quasi-phase-matched second harmonic generation," Opt. Lett. **24**, 1139-1141 (1999).
16. J. U. Kang, Y. J. Ding, W. K. Burns, and J. S. Mellinger, "Backward second-harmonic generation in periodically poled bulk $LiNbO_3$," Opt. Lett. **22**, 862-864 (1997).
17. X. Gu, R. Y. Korotkov, Y. J. Ding, J. U. Kang, and J. B. Khurgin, "Backward second-harmonic generation in periodically poled lithium niobate," J. Opt. Soc. Am. B **15**, 1561-1566 (1998).

#89476 - $15.00 USD Received 6 Nov 2007; revised 19 Dec 2007; accepted 15 Jan 2008; published 31 Jan 2008

18. X. Gu, M. Makarov, Y. J. Ding, J. B. Khurgin, and W. P. Risk, "Backward second-harmonic and third-harmonic generation in a periodically poled potassium titanyl phosphate waveguide," Opt. Lett. **24**, 127-129 (1999).
19. X. Mu, I. B. Zotova, Y. J. Ding, and W. P. Risk, "Backward second-harmonic generation in submicron-period ion-exchanged $KTiOPO_4$ waveguide," Opt. Commun. **181**, 153-159 (2000).
20. C. Canalias, V. Pasiskevicius, M. Fokine, and F. Laurell, "Backward quasi-phase-matched second-harmonic generation in submicrometer periodically poled flux-grown $KTiOPO_4$," Appl. Phys. Lett. **86**, 181105 (2005).
21. M. Conforti, F. Baronio, C. De Angelis, "From femtosecond infrared to picosecond visible pulses: temporal shaping with high-efficiency conversion," Opt. Lett. **32,** 1779 (2007).
22. M. A. Arbore, O. Marco, and M. M. Fejer, "Pulse compression during second-harmonic generation in aperiodic quasi-phase-matching gratings," Opt. Lett. **22,** 865-867 (1997).
23. G. Imeshev, A. Galvanauskas, D. Harter, M. Arbore, M. Proctor, M. Fejer, "Engineerable fs pulse shaping by SHG with Fourier synthetic quasi-phase-matching gratings," Opt. Lett. **23,** 864-864 (1998).
24. G. Imeshev, M. Arbore, M. Fejer, A. Galvanauskas, M. Ferman, D. Harter, "Ultrashort-pulse SHG with nonuniform quasi-phasematching gratings: compression and shaping," J. Opt. Soc. Am. B **17,** 304-318 (2000).
25. U. K. Sapaev and D. T. Reid, "General second-harmonic pulse shaping in grating-engineered quasi-phase-matched nonlinear crystals," Opt. Express **13,** 3264-3276 (2005).
26. U. K. Sapaev and G. Assanto, "Femtosecond pulse synthesis by efficient second-harmonic generation in engineered quasi phase matching gratings," Opt. Express **15,** 7448-7457 (2007).
27. O. Bang, C. B. Clausen, P. L. Christiansen, and L. Torner, "Engineering competing nonlinearities," Opt. Lett. **24,** 1413-1415 (1999).
28. N. C. Kothari, and X. Carlotti, "Transient second harmonic generation: influence of effectiv group-velocity dispersion," J. Opt. Soc. Am. B **5,** 756-764 (1988).
29. E. Sidick, A. Knoesen, and A. Dienes, "Ultrashort-pulse second-harmonic generation. I. Transform-limited fundamental pulses," J. Opt. Soc. Am. B **12,** 1704-1712 (1995).
30. Y. Ding, J. Kang, J. Khurgin, "Theory of backward second-harmonic and third-harmonic generation using laser pulses in quasi-phase-matched 2nd-order nonlinear medium," J. Quantum Electron. **34,** 966-974 (1998).
31. R. Buffa, "Transient second-harmonic generation with spatially nonuniform nonlinear coefficients," Opt. Lett. **27,** 1058-1060 (2002).
32. I. Serban, J. Werschnik, E. Gross, "Optimal control of time-dependent targets," Phys. Rev. A **71**, 053810 (2005).
33. A. Kaiser and V. May, "Optimal control theory with continuously distributed target states: An application to NaK," Chem. Phys. **320,** 95-102 (2006).
34. L. H. Deng, X. M. Gao, Z. S. Cao, W. D. Chen, Y. Q. Yuan, W. J. Zhang, and Z. B. Gong, "Improvement to Sellmeier equation for periodically poled LiNbO3 crystal using mid-infrared difference-frequency generation," Opt. Commun. **268,** 110-114 (2006).

1. Introduction

In a variety of applications, the precise synthesis and manipulation of the profile of optical pulses, i.e. optical pulse shaping, is required. Among others we like to mention spectroscopy, biological imaging, metrology and industrial tests [1-2] The demand for controlled temporal profiles equally applies to all timescales, from femtosecond to pico- and nano-second laser excitations and in various spectral ranges. Shapers should ideally provide high-quality pulses with the desired profiles and (central) wavelength, similar to electronic waveform generators but in distinct time and frequency scales.

To date, conventional picosecond-femtosecond pulse shaping has been implemented using linear effects, for example with free-space bulk optics including diffraction grating pairs and lenses [3]. The drawbacks associated with this approach relate to the need for high-quality optical elements of appreciable size, together with very strict alignment tolerances and the consequently limited integrability with waveguides. In such linear pulse shapers, the input spectrum is modulated (in amplitude and phase) in order to obtain the desired output profile in time. In most cases the input pulse is considered a given constraint and its bandwidth determines the maximum bandwidth of the output. Even though the latter drawback can be overcome using wide bandwidth inputs, this approach often limits the efficiency, inasmuch as desired waveforms of both narrow and large bandwidths can be required from the same input, e.g. in spectroscopy. For instance, the detection of a specific Raman transition might require the shaping of two laser pulses: the Raman pump field (e.g. at 750 nm) with a narrow bandwidth and ps duration; and the

#89476 - $15.00 USD Received 6 Nov 2007; revised 19 Dec 2007; accepted 15 Jan 2008; published 31 Jan 2008

Raman probe with a broadband femtosecond pulse (e.g. from NIR to 750 nm) that stimulates the scattering of a particular vibrational mode [1]. Nowadays, since femtosecond laser sources are available in the wavelength range from 1.3 to 2.0 micrometers, an alternative approach to pulse synthesis in the visible or near-infrared consists in simultaneously frequency doubling and shaping a broadband fundamental frequency (FF) source.

Hereby we propose and numerically demonstrate a novel approach which, starting with a femtosecond near-infrared source, is able to produce and shape both the picosecond Raman pulse and a suitable broadband probe pulse at twice the input frequency. The method is based on Backward Second Harmonic Generation (BSHG) from the fundamental frequency source in an engineered Quasi-Phase-Matching (QPM) grating realized by periodically poling a ferroelectric lithium niobate waveguide.

Over the past decade, BSHG has become a subject of intense investigation ([4] and references therein), owing to a wealth of predicted new phenomena [5, 6] and to the technological progress in fabricating short period QPM gratings [7-10]. Since backward optical parametric oscillation was first proposed in [11], extensive theoretical and experimental studies have been carried out on various backward frequency conversion processes [5-6,11-14]. Experimental demonstration of BSHG with high order QPM was reported in periodically poled lithium niobate and KTP crystals [10,16-20].

In BSHG, since the fundamental and second harmonic (SH) waves propagate in opposite directions, the group velocity mismatch (GVM) plays an essential role in the process of second harmonic generation. In this context, GVM is usually considered a very detrimental effect for the conversion efficiency and, in contrast with the forward SHG case, does not stem from material properties but from the process geometry itself: FF and SH propagate in opposite directions and therefore, even in the absence of material dispersion, GVM is not zero but equal to the sum of the group velocities (V_1 and V_2) of the two waves coupled by the nonlinear process; hence, the temporal walk-off per unit length between FF and SH is $\delta = (1/V_2 + 1/V_1)$. Although GVM is indeed undesired when high doubling efficiencies are sought, in the framework of pulse shaping it can be conveniently exploited to yield and optimize the pulse shaping process. Shaping of second-harmonic pulses has been previously considered in the case of forward SHG [21-26] but never discussed with reference to a backward process, where a huge GVM may allow for shaping possibilities not accessible in forward configurations.

As we will demonstrate in the following, as a general rule of thumb one can think of a shaped output SH generated by a given FF according to two major constraints:
(i) the duration T of the SH pulse is bounded by: $T < \delta L$, being L the length of the structure: e.g. for a 1 mm long lithium niobate sample, the upper bound is of the order of 10 ps. This maximum duration determines the minimum bandwidth B_{SH} of the shaped pulse. In femtosecond stimulated Raman spectroscopy, a small bandwidth is required for the Raman pump because it determines the instrument resolution; typical required values are of the order of $3-17$ cm $^{-1}$, corresponding to transform limited pulses with a few ps duration ($B_{SH}T \geq 0.44$). Note that, for a Lithium Niobate sample, the temporal walk-off per unit length between FF and SH in the backward case is roughly 30 times larger than in the forward case; thus pulse shaping using backward interactions could lead to devices 30 times smaller. For example, if a temporal duration T of 30 ps is envisaged, then a pulse shaper based on forward-SHG would require an unpractical device 10 cm long, while a pulse shaper based on BSHG could be designed using a length of 0.33 cm.
(ii) The bandwidth B_{SH} of the SH pulse is upper bounded by $B_{SH} \leq 2B_{FF}$, being B_{FF} the bandwidth of the FF input.

From a theoretical point of view (i. e. assuming the domain size has no technical limits), in BSHG a fundamental frequency of bandwidth B_{FF} can be shaped into a SH signal with a

#89476 - $15.00 USD Received 6 Nov 2007; revised 19 Dec 2007; accepted 15 Jan 2008; published 31 Jan 2008

maximum bandwidth $2B_{FF}$ (easily up to 2000 cm^{-1}) and a minimum of a few cm^{-1}.

2. Theoretical analysis

In the process of (Type I) second harmonic generation in a non uniform quasi-phase-matching structure, the coupled nonlinear partial differential equations governing the propagation of the complex electric field amplitudes $E_m(z,t)$ ($m=1$ fundamental frequency field FF, $m=2$ second harmonic field SH) of two plane waves of central frequencies ω_m ($\omega_2=2\omega_1$) and wave numbers k_m travelling along the $\pm z$ axis read:

$$i\frac{\partial E_1}{\partial z}=\frac{\beta_1}{2}\frac{\partial^2 E_1}{\partial t^2}-G(z)\exp(-i\Delta kz)E_1^*E_2,\ -i\frac{\partial E_2}{\partial z}=i\delta\frac{\partial E_2}{\partial t}+\frac{\beta_2}{2}\frac{\partial^2 E_2}{\partial t^2}-G(z)\exp(i\Delta kz)E_1^2, \tag{1}$$

with $\Delta k=2k_1+k_2$ being the wave-number mismatch, δ the sum of the inverse group velocities at FF and SH, $\beta_{1,2}$ the group velocity dispersions at FF and SH, respectively. The modulation of the second-order susceptibility is described by the grating function $G(z)$, which represents a square wave with variable duty cycle and period. If the variations of period and duty cycle are slow compared to the spatial frequency of the grating, we can expand $G(z)$ in the Fourier series $G(z)=\chi_0\Sigma_r g_r(z)\exp(irf(z))$ [$\chi_0=\omega d_{eff}/(n_m c)$] and, in the spirit of the rotating–wave approximation, retain only the terms $\pm r$ that are effective (i.e., resonant) to get [27]:

$$i\frac{\partial E_1}{\partial z}=\frac{\beta_1}{2}\frac{\partial^2 E_1}{\partial t^2}-\chi(z)E_1^*E_2,\ -i\frac{\partial E_2}{\partial z}=i\delta\frac{\partial E_2}{\partial t}+\frac{\beta_2}{2}\frac{\partial^2 E_2}{\partial t^2}-\chi^*(z)E_1^2, \tag{2}$$

where $\chi(z)=\chi_0 g_r(z)\exp(irf(z)-i\Delta kz)$.

The coupled equations (2) can be numerically solved with various techniques. Since this is a two boundary problem (the FF input is given in $z=0$ and the SH in $z=L$) we can employ a shooting approach. To solve eqs. (2) in the forward direction we used a fast Fourier transform method and a fourth-order Runge-Kutta routine [28, 29]. First, we calculated BSHG profiles

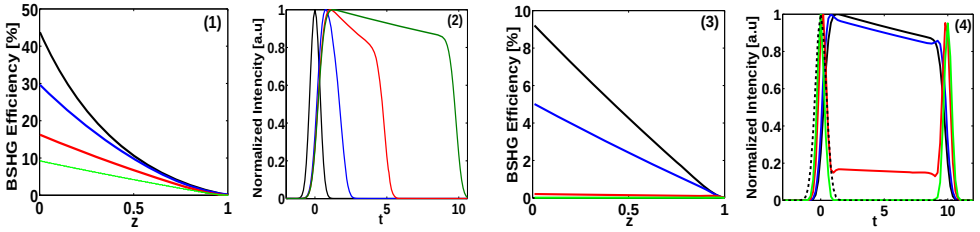

Fig. 1. BSHG conversion efficiency versus z (1) and SH pulse profile (2) (in $z=0$) for perfect QPM ($\Delta k=0$), for various δ: black (δ=0), blue (δ=2), red (δ=5) and green (δ=10). BSHG conversion efficiency versus z (3) and SH pulse profile (4) (in $z=0$) for $\delta=10$ and various Δk: black (Δk=0), blue (Δk=20), red (Δk=50) and green (Δk=100). In (4) the dashed profile is the input FF pulse.

from transform-limited FF inputs in longitudinally uniform (perfectly periodic) QPM gratings. To this extent we set Eqs. 1 in dimensionless format and assumed a unity FF pulse duration (FWHM), $L=1$, $\beta_{1,2}=0$ and $G(z)=1$, respectively. Figure 1(1-2) show the resulting BSHG conversion efficiency vs z and the generated pulses (in $z=0$) for $\Delta k=0$ and various δ. Clearly, the role of GVM in the BSHG process is essential. The temporal profiles of the frequency doubled pulses broaden with δ and the conversion efficiency tends to a linear dependence on

#89476 - $15.00 USD Received 6 Nov 2007; revised 19 Dec 2007; accepted 15 Jan 2008; published 31 Jan 2008

z, in agreement with Ref. [30]. In the case of a mismatched QPM ($\Delta k \neq 0$) and a fixed δ (Fig. 1(3-4)), the results show that Δk severely affects the SH profiles, leading e.g. to splitting for $\Delta k > 50$ (Fig. 1(4)). In the case of interest here, i. e. shaping by BSHG with a non-uniform QPM grating, the control of the output ($z = 0$) SH profile can be stated as follows: having fixed the FF input at $z = 0$, we need to determine the complex function $\chi(z)$ that minimizes the departure of the SH output $[E_2(z = 0,t)]$ from the target pulse shape $[E_{2,target}(t)]$. Once the complex $\chi(z)$ is obtained, we derive the non-uniform QPM modulation able to implement it.

For real functions, to measure the "distance" between target and SH output we use:

$$J_1 = \frac{1}{2}\int_{-\infty}^{+\infty} \left[E_2(z=0,t) - E_{2,target}(t)\right]^2 dt \ . \tag{3}$$

Extending the algorithm described in [21, 31], the problem can be solved by finding the function $\chi(z)$ that minimizes the cost function $J = J_1 + J_2 + c.c.$,[32, 33] where J_1 takes into account the distance from the target and J_2:

$$J_2 = \int_0^L \int_{-\infty}^{+\infty} [\lambda_1 \left(\frac{\partial E_1}{\partial z} + \frac{\beta_1}{2i}\frac{\partial^2 E_1}{\partial t^2} - i\chi E_1^* E_2 \right) - \lambda_2 \left(\frac{\partial E_2}{\partial z} + \delta \frac{\partial E_2}{\partial t} + \frac{\beta_2}{2i}\frac{\partial^2 E_2}{\partial t^2} + i\chi^* E_1^2 \right)] dt dz \tag{4}$$

imposes the fulfillment of eqns. (2); $\lambda_{1,2}(z,t)$ play the role of Lagrange multipliers.
Setting to zero the functional derivatives of J with respect to $\lambda_1(z,t)$, $\lambda_2(z,t)$, $E_1(z,t)$, $E_2(z,t)$, $E_1(z = L,t)$, $E_2(z = 0,t)$, we then get six equations with the functional derivatives with respect to λ_1 and λ_2 providing the evolution equations for FF and SH, namely Eq. (2). The functional derivatives with respect to E_1, E_2 are the evolution equations for the Lagrange multipliers:

$$i\frac{\partial \lambda_1}{\partial z} = -\frac{\beta_1}{2}\frac{\partial^2 \lambda_1}{\partial t^2} - \chi^* \left(\lambda_1^* E_2^* - 2\lambda_2 E_1\right), -i\frac{\partial \lambda_2}{\partial z} = i\delta \frac{\partial \lambda_2}{\partial t} - \frac{\beta_2}{2}\frac{\partial^2 \lambda_2}{\partial t^2} + \chi \lambda_1 E_1^* . \tag{5}$$

Finally, the functional derivatives with respect to $E_1(z = L,t)$, $E_2(z = 0,t)$ give the boundary conditions for Eq. (5): $\lambda_1(z = L,t) = 0$ and $\lambda_2(z = 0,t) = -[E_2(z = 0,t) - E_{2,target}(t)]$.
Using the functional derivative with respect to $\chi(z)$:

$$\frac{\delta J}{\delta \chi} = \int_{-\infty}^{\infty} \left(-i\lambda_1 E_2 E_1^* + i\lambda_2^* E_1^{2*}\right) dt. \tag{6}$$

we update the algorithm and determine the optimum $\chi(z)$ by the procedure:

I: choose an initial guess for $\chi(z)$ and solve Eqs. (2);

II: use the results obtained in the previous step to solve the evolution equations for the Lagrange multipliers (Eqs. (5));

III: update $\chi(z)$: $\chi(z) \leftarrow \chi(z) + \alpha \frac{\delta J}{\delta \chi}$, with α a suitable constant;

IV: if/when the obtained result is close enough to the target, the iterative procedure stops, otherwise it goes back to point 2.

Once the optimal nonlinear profile is found (i. e. we obtained the function $\chi(z)$ that minimizes the distance J_1 between target and SH output), the QPM can be implemented by assuming the use an r-order grating and considering only its r-th Fourier coefficient, i.e. $g_r(z) = \frac{2}{r\pi}\sin(\pi r d_c(z))\exp[-ir\pi d_c(z)]$, from which we get the duty cycle $d_c(z)$ and the period Λ of the square modulation:

$$d_c(z) = \frac{1}{r\pi}\arcsin\left(\pm\frac{r\pi}{2}\frac{|\chi(z)|}{\chi_0}\right), \Lambda(z) = r2\pi\left(\Delta k + \frac{d\left[\mathrm{Arg}[\chi(z)] + r\pi d_c(z)\right]}{dz}\right)^{-1} . \tag{7}$$

#89476 - $15.00 USD Received 6 Nov 2007; revised 19 Dec 2007; accepted 15 Jan 2008; published 31 Jan 2008

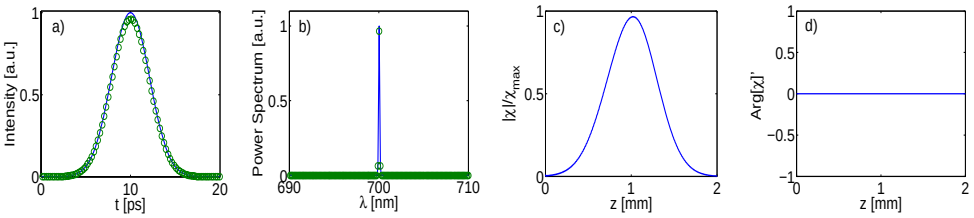

Fig. 2. (a) SH output (circles) and target (solid line) intensity profiles versus time. (b) SH output (circles) and target (solid line) spectral intensities. (c) Amplitude of the optimal nonlinearity distribution. (d) Derivative of the argument of the complex nonlinear coefficient, related to the residual wavevector mismatch (see eq.(7)).

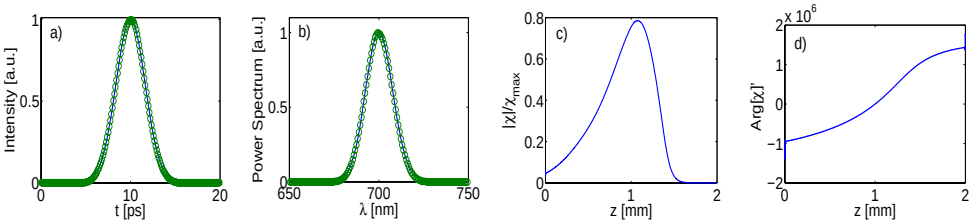

Fig. 3. Same as in Fig. 2, but for a chirped SH target pulse and a 10% conversion efficiency.

3. Results and discussion

To demonstrate the method, we consider $L = 2\,mm$ periodically poled lithium niobate (PPLN) crystals for which $\chi_0 = 6.35 \cdot 10^{-5} V^{-1}$, $\delta \approx -100 \cdot 10^{-10} s/m$, $\beta_1 \approx 1.5 \cdot 10^{-25} s^2/m$ and $\beta_2 \approx 4.5 \cdot 10^{-25} s^2/m$. [34] We took a transform limited FF gaussian input with peak intensity $I = 20\,GW/cm^2$ and full width at half maximum (FWHM) $T_{FF} = 40\,fs$, centered in $\lambda = 1400\,nm$. Since the dispersion length for the pump pulse is considerably larger than the sample length, we can neglect dispersion effects.

As a first target, we choose a transform limited SH gaussian pulse with FWHM $T_{FF} = 5\,ps$ and a conversion efficiency of 20%. Figure 2(a) displays the output SH intensity (circles) compared to the target (solid line): the agreement is perfect (after 100 iterations the relative error is $< 10^{-4}$). Fig. 2(b) graphs the output SH spectrum, transform limited with a bandwidth of $0.14\,nm$ ($2.9\,cm^{-1}$). Figure 2(c) plots the normalized amplitude of the nonlinear coefficient $\chi(z)$. Since we sought a transform limited (i.e. real) target and neglected dispersion, the nonlinear coefficient is purely real, as visible also in Fig. 2(d).

Next, we consider a chirped gaussian SH pulse with bandwidth equal to a transform limited SH pulse of duration $T_{SH} = 40\,fs$ and a 10% conversion efficiency. A long chirped SH target (rather than short and transform-limited) allows us to use the entire length of the crystal for frequency conversion. In such a way the maximum conversion efficiency, ultimately limited by the maximum value of the nonlinear coefficient, can be significantly enhanced. Figure 3(a) shows the agreement between SH output (circles) and target (solid line) pulses. Fig. 3(b) displays the output SH spectra, with a wide bandwidth of about $20\,nm$ FWHM (i.e., $400\,cm^{-1}$).

Let us now address the feasibility of the proposed devices. The current state of the art on periodic poling of Lithium Niobate allows for the realization of domain lengths as short as $200nm$

#89476 - $15.00 USD Received 6 Nov 2007; revised 19 Dec 2007; accepted 15 Jan 2008; published 31 Jan 2008

[8]. In our examples, the implementation of the grating exploiting first-order QPM would require minimum domain lengths of about $65nm$. This value appears to be well within reach thanks to the continuous progress in poling technology for ferroelectric crystals. The requirement on minimum pitch, however, could be relaxed by using higher-order QPM at the expense of conversion efficiency. For example, the target of Fig. 2 can be obtained with second-order QPM if we use a peak excitation of $40GW/cm^2$ and limit the conversion efficiency to 10%: with the latter specifications the minimum domain length would be $100nm$.
Finally, considering the device sensitivity to fluctuations in input characteristics (i.e. intensity, chirp and duration), we verified that the design is rather robust against such variations, the effects of them on the output pulses being substantially limited to slight changes in amplitude (i.e. conversion efficiency) and shape.

4. Conclusions

By using Lagrange multipliers and shooting we demonstrated that pulse shaping can be achieved by engineering the domain distribution of a Quasi-Phase-Matching grating for backward SHG, exploiting the large group-velocity-mismatch. These results, contemporary relevant due to the progress in short-period poling of ferroelectrics and the interest in counterpropagating wave mixing, enrich the applicative scenario of backward three-wave interactions.

Acknowledgments

This work was supported by the Italian MUR (PRIN 2005098337) and the EU (POISE, RTN no. 512450).

#89476 - $15.00 USD Received 6 Nov 2007; revised 19 Dec 2007; accepted 15 Jan 2008; published 31 Jan 2008